Extreme hydrogen plasma densities achieved in a linear plasma generator

DOI:
10.1063/1.2716208

Document status and date:
Published: 01/01/2007

Document Version:
Publisher's PDF, also known as Version of Record (includes final page, issue and volume numbers)

Extreme hydrogen plasma densities achieved in a linear plasma generator

G. J. van Rooij,[a] V. P. Veremiyenko, W. J. Goedheer, B. de Groot, A. W. Kleyn, P. H. M. Smeets, and T. W. Versloot
FOM-Institute for Plasma Physics Rijnhuizen, Association EURATOM-FOM, Trilateral Euregio Cluster, Nieuwegein, Uthrecht 3430BE, The Netherlands

D. G. Whyte
Massachusetts Institute of Technology, Cambridge, Massachusetts 02139-4307

R. Engeln, D. C. Schram, and N. J. Lopes Cardozo
FOM-Institute for Plasma Physics Rijnhuizen, Association EURATOM-FOM, Trilateral Euregio Cluster, Nieuwegein, Uthrecht 3430BE, The Netherlands and Eindhoven University of Technology, 5600 MB Eindhoven, The Netherlands

(Received 5 October 2006; accepted 18 February 2007; published online 23 March 2007)

A magnetized hydrogen plasma beam was generated with a cascaded arc, expanding in a vacuum vessel at an axial magnetic field of up to 1.6 T. Its characteristics were measured at a distance of 4 cm from the nozzle: up to a 2 cm beam diameter, 7.5×10^{20} m^{-3} electron density, ~2 eV electron and ion temperatures, and 3.5 km/s axial plasma velocity. This gives a 2.6×10^{24} H^{+} m^{-2} s^{-1} peak ion flux density, which is unprecedented in linear plasma generators. The high efficiency of the source is obtained by the combined action of the magnetic field and an optimized nozzle geometry. This is interpreted as a cross-field return current that leads to power dissipation in the beam just outside the source. © *2007 American Institute of Physics*. [DOI: 10.1063/1.2716208]

Production of high density low temperature hydrogen plasma is the key ingredient of a laboratory experiment for studies on "plasma surface interaction" (PSI) under conditions relevant for the divertor of ITER.[1] Fusion reactors such as ITER confine a plasma of hydrogen isotopes at >15 keV using magnetic fields. Their field topology causes the outer layer of the plasma to exhaust to a special area of the plasma chamber, the divertor, where it is neutralized and pumped away. The particle and energy fluxes to the strike zones in the divertor are dictated by the transport from the hot plasma core. The numbers that are foreseen for ITER are 10^{24} ions m^{-2} s^{-1} and 10 MW m^{-2} to the strike zones in the divertor.[2] This corresponds to a plasma density close to the wall of 10^{21} m^{-3} at a temperature of a few eV. A surface that can handle such fluxes in steady state is a major research challenge for fusion reactors and a priority for ITER.

Even the largest present day fusion experiments cannot easily realize such extreme divertor plasma conditions, especially not for long exposure times. There are several linear plasma generators[3–5] that study PSI, but the simultaneous achievement of high hydrogen ion density and low temperature is outside of their capability. Only inside high pressure discharges, such as the cascaded arc, are these conditions routinely produced.[6] However, transfer of the plasma to low pressure conditions (~1 Pa) without losing the high density had never been accomplished until now.

In this letter, we report on a series of experiments in the linear plasma generator Pilot-PSI (see Fig. 1 and caption for the experimental details), in which we do realize the plasma densities that are expected in the ITER divertor. We used strong magnetic fields (up to 1.6 T) to confine the output of a cascaded arc, thus generating intense magnetized hydrogen plasma beams. We based the design of the cascaded arc on extensive work at the Eindhoven University of Technology.[8] There operation in hydrogen was shown to be limited to low plasma densities (typically $n_e<10^{19}$)[9,10] due to recombination with molecular hydrogen.[11] This letter demonstrates that it is possible to get much higher densities by operating the source in a strong magnetic field, at a higher discharge current, with a lower neutral pressure in the vessel, and by using different nozzle geometries.

The experimental approach consisted of two elements: (i) variation of the geometry of the source and (ii) scan of the axial B field. The results demonstrated that the combined

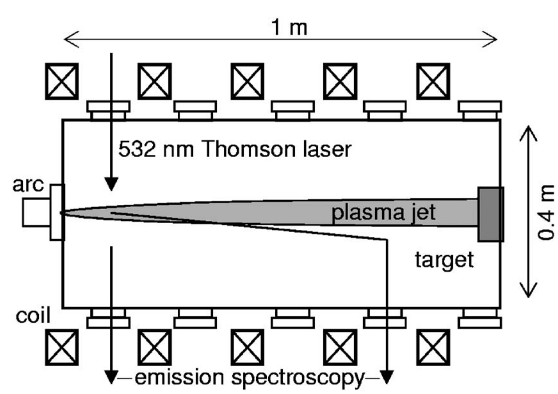

FIG. 1. Schematic drawing of Pilot-PSI. A 1 m long 0.4 m diameter vacuum vessel (pumped to ~1 Pa) is placed inside five coils that produce an axial magnetic field up to ≤1.6 T. The cascaded arc exhausts plasma into the vessel along the magnetic field axis. It consisted of three tungsten cathodes in a cathode chamber, a stack of five insulated copper plates with a 4 mm hole that forms the 30 mm length discharge channel, and a copper tungsten nozzle that also serves as anode. The inner diameter of the leading 4 mm was varied between ∅5 and ∅8 mm and followed by a preexpansion section of 15 mm × ∅16 mm. The source was operated on hydrogen with a gas flow of 2.5 SLM=1.0×10^{21} H_2/s and a discharge current of 100 A. This sets the cathode chamber pressure to 10^4 Pa. Due to the high collisionality the Saha equilibrium fixes the temperature at $kT\sim1.3$ eV. (Ref. 7). At the exit of the plasma channel the plasma flows at sound speed (Mach=1 boundary condition) and expands into the vessel.

[a]Electronic mail: rooij@rijnh.nl

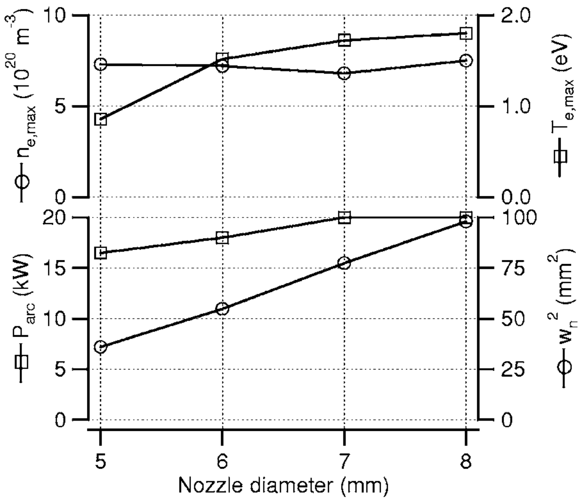

FIG. 2. $n_{e,\max}$ and $T_{e,\max}$ (upper panel) and discharge power and w_n^2 (lower panel) vs nozzle diameter at B=1.6 T. The plasma output (proportional to w_n^2) increases much more than the input power, hence the source becomes more efficient at larger nozzle diameter.

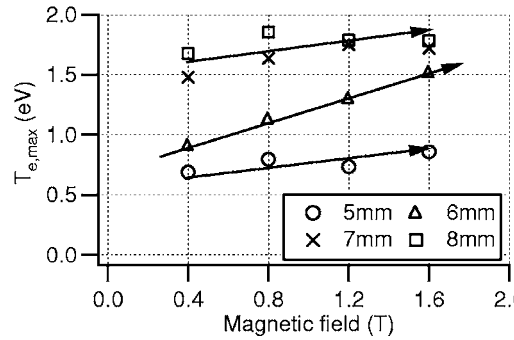

FIG. 3. Effect of the nozzle geometry on the electron temperature for a scan of the magnetic field. The arrows are drawn to guide the eye and to point to the two regimes that are crossed by the 6 mm nozzle.

effect of an optimized source geometry and application of a strong B-field lead to an extreme improvement of the hydrogen plasma production. Having established that ITER-like conditions can be reached, we address the following issues: (i) efficiency of the source; (ii) mechanism of the efficient plasma production, synergy of the strong B field and source geometry; (iii) equilibration of electron and ion temperatures.

Profiles of n_e and T_e were measured with Thomson scattering at 40 mm from the nozzle (well outside of the source). The scattered light was collected from 30 laser shots with an array of fibers to simultaneously obtain radial profiles over an observational chord of 25 mm. The profiles were fitted with bell-shaped curves and characterized by their peak values ($n_{e,\max}$, $T_{e,\max}$) and widths w_n, w_T (full width at half maximum). The T_e profiles are wider than the n_e profiles in all cases, hence we use w_n to characterize the width of the plasma beam. To determine the flux density in the plasma beam, the Doppler shift of the $\boldsymbol{H}_\beta$ line was measured with high-resolution spectroscopy, using a small viewing angle with respect to the axis. v_{axial}=3.5 km/s was found at 40 mm from the nozzle for all field settings. Line profiles were also measured for a perpendicular viewing line to determine the ion temperature and plasma rotation velocity.

The effect of the nozzle diameter on the plasma production was studied for diameters of between 5 and 8 mm at B=1.6 T. Figure 2 summarizes the results. It shows that $T_{e,\max}$ increases from 0.8 to 1.8 eV, going from a 5 mm nozzle to 8 mm. It is recalled (see caption Fig. 1) that $T_{e,\max}$ inside the plasma channel must expected to be ~1.3 eV. This means that the plasma cools between the source and measuring volume for a narrow nozzle, whereas with the wide nozzle there is even postheating. In contrast, $n_{e,\max}$ is not dependent on the nozzle diameter. Hence, the plasma output of the source is proportional to w_n^2, which does rise steeply with the nozzle size. The increase of the nozzle diameter also leads to an increase of the power dissipated in the source. Measurements of the voltage at the individual plates showed that this increase is entirely due to increase of the voltage between the last cascade plate and the nozzle. For B=1.6 T this voltage increases from 55 V for the 5 mm nozzle to 100 V for the 8 mm nozzle. The magnetic field is an important parameter here: at B=0.4 T these voltages are 20 and 35 V, respectively. The increased voltage between the last plate and the nozzle indicates that the wider nozzle gives rise to a significant Ohmic power dissipation in a region of the plasma beam that is effectively already outside of the source. Here, the neutral density is decreased and the power loss to the wall is strongly reduced. This is in agreement with the observed temperatures, which are higher than inside the plasma channel. In addition, the modified nozzle geometry suppresses plasma losses at the nozzle surface due to surface recombination, which was already identified as an important loss mechanism by Vankan *et al.* in experiments without magnetic field.[10] Ongoing experiments in which fast images (exposure time of ~100 ns) are taken of the visible light emitted from the nozzle region support this view. These show a cylindrical channel of ~5 mm diameter that attaches to the nozzle and that extends up to centimeters into the vessel. This channel rotates at 10–100 kHz around the plasma column.

In Fig. 3, $T_{e,\max}$ is plotted against B for the different nozzle diameters. This plot suggest the existence of two regimes as indicated by the arrows. A low T_e regime is observed at around 0.9 eV for the smaller diameters and $T_e > 1.6$ eV is measured for the larger diameters. A transition between the two regimes is observed for the 6 mm nozzle. The balance between net heating and cooling is determined by the combination of plasma confinement and nozzle diameter.

Having established the beneficial effect of the wide nozzle, which leads to postheating of the beam after it has exited the source, we investigate the effect of the magnetic field for the fixed nozzle diameter of 8 mm. Figure 4 shows $n_{e,\max}$ and the ionization efficiency. Striking is the linear increase of $n_{e,\max}$ with B, reaching values in excess of 7.5×10^{20} m^{-3} at B=1.6 T. At B=0 T, $n_{e,\max}$ was below the Thomson scattering detection limit, i.e., $n_e < 10^{19}$ m^{-3}. Multiplying the n_e profile with the axial velocity of 3.5 km/s yields a peak flux density of 2.6×10^{24} H$^+$ m^{-2} s^{-1}. Integrating over the flux density profile and normalizing this to the input gas flow yield the total ionization efficiency of the source, which reaches 16% at 1.6 T. Hence, the combined effect of the wide nozzle and the strong magnetic field has made it possible to achieve a plasma beam which is in density, temperature, and flux density in the parameter range of the ITER divertor plasma. The net power efficiency, i.e., the total power in the beam (kinetic, ionization, and dissociation

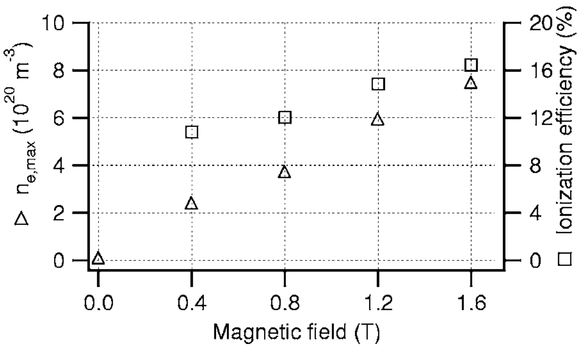

FIG. 4. $n_{e,\max}$ (squares, left axis) and ionization efficiency (triangles, right axis) measured for the 8 mm nozzle.

energy) divided by the total power input in the source, is as large as 5%. The T_e profiles do not change significantly in the range $B=0.4-1.6$ T. The difference is large compared to $B=0$ T: $T_e=0.2-0.5$ eV at $B=0$ T was measured with a Langmuir probe.

Downstream from the nozzle n_e decreased and we observed values for T_e that differed from the in-source T_e. High-resolution spectroscopy was performed to investigate if the ion temperature T_i was still coupled to T_e. The line broadening of Balmer β light collected perpendicularly to the plasma jet was measured at $B=0.4$ T (i.e., the lowest density conditions, hence the lowest collisionality) for the 8 mm nozzle. In fact, this gives the temperature of the neutral atoms T_0. The excited atoms may thermalize with the ions via charge exchange: $H(n=4)+H^+ \rightleftarrows H^+ + H(n=4)$. In this process, a single collision is sufficient to transfer the ion temperature and velocity to the atoms. We estimate that this process is important because the typical lifetime of the $n=4$ level $[(3-6)\times 10^{-8}$ s (Ref. 12)] is long compared to the time constant for charge exchange of 8×10^{-9} s [reaction rate at 1 eV, $k=3\times 10^{-13}$ $m^3\,s^{-1}$ (Ref. 12) times n_e at $B=0.4$ T$=4\times 10^{20}$ m^{-3}]. Deconvolution of the Doppler and Stark component yielded a neutral atom temperature of $T_0\sim 2$ eV. Comparison with $T_e\sim 1.7$ eV (Fig. 3) confirms the coupling.

The voltage between the last plate and the nozzle, that was measured to increase with B up to 100 V, implies radial electrical fields of up to 25 kV/m. This will induce fast rotation of the plasma jet via the $\mathbf{E}\times\mathbf{B}$ drift. Ongoing investigations with emission spectroscopy indeed indicate rotation velocities approaching the acoustic velocity, which possibly lead to viscous heating of the ions.

We conclude that the high efficiency achieved in these experiments is the result of the synergy between the wide nozzle and the strong magnetic field. We demonstrated that this combination leads to significant power dissipation in the plasma outside the source. Plasma confinement inside a wide nozzle means that the current crosses the B field through a thicker and colder plasma region, i.e., a higher resistivity and more power dissipation. This enhances the ionization degree and thereby the density. Finally, the ionization degree inside the source is predicted to be maximally 10%.[13] The measured 16% ionization efficiency again supports postsource heating. By virtue of this nozzle-field synergy, a plasma hydrogen jet was produced with $n_e=7.5\times 10^{20}$ m^{-3} and $T_e\sim 2$ eV, reaching a maximum flux density of 2.6×10^{24} $H^+\,m^{-2}\,s^{-1}$. These plasma parameters are in the ITER divertor range and open a window on PSI studies in conditions relevant to fusion reactors.

This work, supported by the European Communities under the contract of Association between EURATOM/FOM, was carried out within the framework of the European Fusion Programme with financial support from NWO.

[1] ITER Physics Basis, Nucl. Fusion **39**, 2137 (1999).
[2] G. Federici, P. Andrew, P. Barabaschi, J. Brooks, R. Doerner, A. Geier, A. Herrmann, G. Janeschitz, K. Krieger, A. Kukushkin, A. Loarte, R. Neu, G. Saibene, M. Shimada, G. Strohmayer, and M. Sugihara, J. Nucl. Mater. **313-316**, 11 (2003).
[3] G. Y. Antar, Phys. Rev. Lett. **87**, 065001 (2001).
[4] N. Ohno, N. Ezumi, S. Takamura, S. I. Krashininnikov, and A. Yu. Pigarov, Phys. Rev. Lett. **81**, 818 (1998).
[5] H. Meyer, S. Klose, E. Pasch, and G. Fussmann, Phys. Rev. E **61**, 4347 (2000).
[6] D. C. Schram, Nucl. Instrum. Methods Phys. Res. B **139**, 136 (1998).
[7] R. P. Dahiya, M. J. de Graaf, R. J. Severens, H. Swelsen, M. C. M. van de Sanden, and D. C. Schram, Phys. Plasmas **1**, 2086 (1994).
[8] M. C. M. van de Sanden, J. M. de Regt, G. M. Janssen, J. A. M. van der Mullen, D. C. Schram, and B. van der Sijde, Rev. Sci. Instrum. **63**, 3369 (1992).
[9] R. F. G. Meulenbroeks, D. C. Schram, M. C. M. van de Sanden, and J. A. M. van der Mullen, Phys. Rev. Lett. **76**, 1840 (1996).
[10] P. Vankan, R. Engeln, and D. C. Schram, Appl. Phys. Lett. **86**, 101501 (2005).
[11] M. J. de Graaf, R. Severens, R. P. Dahiya, M. C. M. van de Sanden, and D. C. Schram, Phys. Rev. E **48**, 2098 (1993).
[12] R. K. Janev, W. D. Langer, K. Evans, Jr., and D. E. Post, Jr., *Elementary Processes in Hydrogen-Helium Plasmas* (Springer, Berlin Heidelberg, 1987).
[13] K. T. A. L. Burm, W. J. Goedheer, J. A. M. van der Mullen, G. M. Janssen, and D. C. Schram, Plasma Sources Sci. Technol. **7**, 395 (1998).